Contribution from the Chemistry Division,
Argonne National Laboratory, Argonne, Illinois 60439

Structural Studies of Precursor and Partially Oxidized Conducting Complexes. 1. A Neutron Diffraction and Spectroscopic Investigation of Quasi-One-Dimensional Potassium Tetracyanoplatinate (1.75:1) Sesquihydrate, $K_{1.75}[Pt(CN)_4]\cdot 1.5H_2O$[1]

JACK M. WILLIAMS,* KEITH D. KEEFER, DONALD M. WASHECHECK, and NANCY P. ENRIGHT[2]

Received March 22, 1976 AIC601986

The complete molecular structure of quasi-one-dimensional, partially oxidized potassium tetracyanoplatinate (1.75:1) sesquihydrate, $K_{1.75}[Pt(CN)_4]\cdot 1.5H_2O$, has been determined by a single-crystal neutron diffraction study. The potassium *deficient* tetracyanoplatinate, K(def)TCP hereafter, crystallizes with four formula units in the triclinic unit cell C_i^1-$P\bar{1}$, with cell constants $a = 10.360$ (17) Å, $b = 9.303$ (15) Å, $c = 11.832$ (19) Å, $\alpha = 77.57$ (9)°, $\beta = 114.74$ (5)°, and $\gamma = 73.64$ (7)°. A total of 5037 observed data were averaged to yield 3969 independent reflections (3276 data with $F_o^2 > \sigma F_o^2$). The structure was solved from the neutron Patterson map and refinement using full-matrix least-squares techniques has led to an agreement factor of $R(F_o^2) = 0.058$. The agreement factor for 3276 data with $F_o^2 > \sigma F_o^2$ is $R(F_o^2) = 0.054$. The structure comprises an unusual "zig-zag" metal atom chain containing three crystallographically independent Pt atoms with a Pt(1)–Pt(2)–Pt(3) bond angle of 173.25 (3)°. Inversion centers occur at Pt(1) and Pt(3). The most surprising finding is that the two independent metal atom separations are *equal* [2.961 (1) and 2.965 (1) Å], though not required to be so by symmetry, just as in the case of $K_2[Pt(CN)_4]Br_{0.3}\cdot 3H_2O$ where they are 2.888 (6) Å and 2.892 (6) Å. The short Pt–Pt separations and almost totally *non*-eclipsed configuration of adjacent $Pt(CN)_4^{-1.75}$ groups (torsion angles between adjacent platinocyanide groups ranging from 38.46 to 51.82°) are indicative of considerable $Pt(5d_{z^2})$ metal overlap, strong metal–metal bond formation, and repulsive π–π cyanide interactions. While Pt(1) and Pt(3) reside on the *c* axis, Pt(2) is displaced 0.170 (1) Å normal to *c*. The deformation of the Pt atom chain is the result of an asymmetric electrostatic environment about Pt(2) involving $K^+\cdots{}^-N{\equiv}C$ interactions. Although the CN groups of Pt(2) form the greatest number (and shortest O–H···N contacts) of water molecule to cyanide hydrogen bonds, the Pt chain deformation is *not* due to $C{\equiv}N^-\cdots H_2O$ hydrogen bond formation. The water molecules play an important role in the structure of the crystal, i.e., in addition to forming single and bifurcated hydrogen bonds, which bind adjacent $Pt(CN)_4^{-1.75}$ groups in a single strand of a Pt–Pt chain, they also serve to cross-link $Pt(CN)_4^{-1.75}$ groups of different $Pt(CN)_4^{-1.75}$ stacks. In addition to normal H-bonding interactions, all lone-pair orbitals appear to be directed toward K^+ ions, increasing the binding of the water molecules. Also involved in the overall hydrogen bonding scheme is a disorder of one K^+ ion and one H_2O molecule. We have found no evidence for formation of an incommensurate superlattice. It appears that the Pt chain deformation originates in the asymmetric electrostatic lattice interactions and is not caused either by a charge density wave or a Peierls distortion. Preliminary results from neutron inelastic scattering studies confirm that strong electron–phonon coupling exists in K(def)TCP; polarized specular reflectance data also indicate this salt is a "one-dimensional" metal at room temperature. The neutron inelastic scattering results are in accord with ongoing diffuse x-ray scattering experiments which confirm the existence of a Kohn anomaly in K(def)TCP. Crystal structure modifications now in progress are discussed which will, in principle, result in restoration of the Pt chain linearity in these cation deficient complexes and hopefully lead to enhanced metallic conductivity.

Introduction

Partially oxidized one- and quasi-one-dimensional (1-D) cyanoplatinate compounds continue to attract strong interest because of their high, nearly metallic electrical conductivities and they provide experimental results which greatly aid in the development of the theory of the one-dimensional state. The 1-D properties arise from the Pt atom "chains" formed in these compounds. The high conductivity is a result of short metal–metal separations within a chain allowing intrachain valence electron delocalization.

The one-dimensional conduction properties and associated phenomena, such as Peierls' distortions and charge density wave displacements, are all influenced to some degree by the crystalline environment of the metal–atom chains, viz., ligands, cations, anions, and lattice water molecules. We have undertaken a program of materials synthesis and detailed characterization of a wide range of one-dimensional compounds and their starting products. We are determining both the qualitative and quantitative effects of chemical and environmental factors on the conductivity of these compounds. With this knowledge, chemical modifications have then been undertaken in order to amplify the most unusual properties of these novel compounds.

The prototype compounds of this group are the *anion* deficient derivatives $K_2[Pt(CN)_4]X_{0.3}\cdot 3H_2O$, referred to as KCP(Br) and KCP(Cl) where X is Br^- or Cl^-, respectively. We have recently reported revised structures for KCP(Br)[3] and KCP(Cl)[4] determined using single-crystal neutron diffraction techniques. Both of these structures contain an essential anion disorder resulting from the halide ion nonstoichiometry. The corresponding *cation* deficient tetracyanoplatinates provide a new structural modification and we recently reported the preliminary results of a neutron diffraction study[5] of $K_{1.75}[Pt(CN)_4]\cdot 1.5H_2O$, K(def)TCP. This metallic appearing salt contains a very unusual "zig-zag" Pt atom chain; hence, it is referred to as being a quasi-one-dimensional chain.

In this paper we discuss the detailed chemical and molecular structure of K(def)TCP and the origin of the Pt chain distortion and present new information dealing with a K^+–H_2O disorder which we have discovered upon further analysis of our neutron diffraction data. A recent single crystal x-ray analysis[6] of $K_{1.75}[Pt(CN)_4]\cdot 1.5H_2O$ has also appeared which is in essential agreement with our findings. Finally we present structural comparisons between partially oxidized $K_2[Pt(CN)_4]Br_{0.3}\cdot 3.0H_2O$, $K_{1.75}[Pt(CN)_4]\cdot 1.5H_2O$, and the unoxidized starting product[7] $K_2[Pt(CN)_4]\cdot 3H_2O$ which we have recently studied. From an analysis of these structural comparisons we predict the synthetic chemical modifications necessary to alter the Pt chain deformation in these compounds and enhance 1-D conductivity.

Experimental Section

Crystal Preparation. After preparation of $K_{1.75}[Pt(CN)_4]\cdot 1.5H_2O$ using a modified method outlined by Levy,[8,9] crystals were grown by slow evaporation of a saturated aqueous solution in a desiccator over

Table I.[a] Published Structural Data on $K_{1.75}[Pt(CN)_4]\cdot 1.5H_2O$

Compd formulation	Cell data: Crystal system	a, Å; α, deg	b, Å; β, deg	c, Å; λ, deg	ρ_{obsd}, g/cm³; ρ_{calcd}, g/cm³	V_{cell}, Å³	Pt–Pt separation, Å	Ref
$K_7Pt_4(CN)_{16}\cdot 6H_2O$[b] or $K_{1.75}[Pt(CN)_4]\cdot 1.5H_2O$								Levy[8] (1912)
$K_{1.74}[Pt(CN)_4]\cdot 1.8H_2O$	Triclinic[c]	15.59 92.5	10.01 92.5	2.96 92.1	2.79 2.87	460.6	2.96 (c length)	Krogmann and Hausen[10] (1968)
$K_{1.78}[Pt(CN)_4]Br_{0.034}\cdot 2H_2O$	Triclinic[d]	10.32 (1) 102.6 (1)	11.80 (1) 106.2 (1)	9.29 (1) 114.8 (1)		910.4	2.95 (b/4 length)	Minot et al.[12] (1973)
$K_{1.75}[Pt(CN)_4]\cdot 1.5H_2O$	Triclinic[e] [C_i^1-$P\bar{1}$] [$Z = 4$]	10.36 (2) 102.4 (1)	11.83 (2) 106.4 (1)	9.30 (2) 114.7 (1)	2.82 (1) 2.85	918.3	2.96 (b/4 length)	This work

[a] The estimated standard deviations are given in parentheses and refer to the least-significant figures. [b] Original formulation by Levy.[8] [c] Powder x-ray diffraction data; faint lines referred to as "superlattice" lines indicate c axis length should be doubled (5.92 Å). [d] Single crystal x-ray data. Triclinic cell data are those for the primitive Delauney-reduced cell. [e] Single crystal neutron data. Data for the primitive Delauney-reduced cell are given. X-ray powder patterns of this material are identical to that reported by Krogmann and Hausen[10] hence all materials reported in this table appear to have the same molecular structure. The transform of $a' = a - b + {}^1/_2c$; $b' = a + b + {}^1/_4c$; and $c' = {}^1/_4c$ gives the cell $a' = 15.592$, $b' = 9.979$, $c' = 2.958$, $\alpha' = 87.70$, $\beta' = 92.42$, $\gamma' = 87.89$ where a, b, and c refer to the cell in which data were collected.

magnesium perchlorate. This procedure yielded well-formed, bronze-colored crystals with dimensions typically 1–2 mm on a side and up to 30 mm in length.

The compound $K_{1.75}[Pt(CN)_4]\cdot 1.5H_2O$ has been given various formulations as shown in Table I; however, from our work (vide infra) it is clear that all of these materials are structurally identical. First, although none of the unit cell constants reported in Table I match those of Krogmann and Hausen,[10] powder x-ray diffraction patterns of our crystals and of material prepared by Miller[11] agree perfectly with that published by Krogmann and Hausen.[10] The Krogmann and Hausen unit cell may be derived from the cell reported in this work by considering it to consist only of Pt atoms and allowing $c/4$ translations as valid translational symmetry operations. This is not precisely true; however, x-ray powder patterns exhibit this pseudo-symmetry. The transformation equation is given in Table I. Second, the triclinic Delauney-reduced cell parameters, which we have derived from our single crystal observations, are identical to those reported by Minot et al.[12] The latter also reported the presence of a slight amount of Br^- in their material. Chemical analysis[13] of our material for C, H, N, and halogen shows very good agreement with that obtained from our diffraction study. We have found that a trace of halogen (<1.0%) is sometimes observed in the chemical analysis of $K_{1.75}[Pt(CN)_4]\cdot 1.5H_2O$ originating from the $K_2[Pt(CN)_4]\cdot 3H_2O$ starting material; when the latter is purified repeatedly until no halogen is detected the $K_{1.75}[Pt(CN)_4]\cdot 1.5H_2O$ is obtained halogen free.[9] Final Fourier difference density maps, in which correct phasing of F_o is achieved using the disordered model reported herein, are virtually featureless giving no indication of a possible halide position.

Unit Cell and Space Group. From x-ray diffraction precession and Weissenberg photographs, it was demonstrated that K(def)TCP is triclinic. However, the x-ray photographs were misleading in that one axis appeared to be extremely short ($c \simeq 2.96$ Å). It also appeared that a few very weak spots might indicate the presence of an "incommensurate" superlattice. However, when the crystals were examined using neutrons, a case in which the dominant scattering of Pt is nullified, it was revealed that the cell derived from x-ray observations was misindexed: c was actually of a length four times that originally derived. Because of this scattering dominance of Pt, x-ray examinations of this salt can be extremely misleading due to the virtually equal spacing of the platinum atoms which causes false translational symmetry in the x-ray photographs.

The lattice parameters for the triclinic cell were determined from 28 intense reflections, ranging in 2θ from 40 to 60°, which were automatically centered on the neutron diffractometer.[15] A least-squares fit of the angles 2θ, X, and ϕ of these reflections, measured at 22 ± 2 °C with a neutron wavelength of 1.142 (1) Å, yielded a = 10.360 (17) Å, b = 9.303 (15) Å, c = 11.832 (19) Å, α = 77.57 (9)°, β = 114.74 (5)°, γ = 73.64 (7)°, and V_c = 918.3 Å³. Calibration of the neutron wavelength was made with two standard cubic crystals: NaCl (a = 5.6397 Å) and Si (a = 5.4308 Å) at 22 ± 2 °C. Delauney-reduced cell parameters were derived using the computer program "TRACER II"[16] and are a' = 10.36 Å, b' = 11.83 Å, c' = 9.30 Å, α' = 102.4°, β' = 106.4°, and γ' = 114.7°. The base vectors for the unreduced cell are related to those of the Delauney-reduced cell by the transformation

$$\begin{pmatrix} a' \\ b' \\ c' \end{pmatrix} = \begin{pmatrix} 1 & 0 & 0 \\ 0 & 0 & 1 \\ 0 & \bar{1} & 0 \end{pmatrix} \begin{pmatrix} a \\ b \\ c \end{pmatrix}$$

The crystal density of 2.82 (1) g cm^{-3}, determined by flotation, agrees well with the calculated value of 2.85 g cm^{-3} based on four formula units per unit cell.

Data Collection. A well-formed bronze-colored crystal of approximate dimensions 1.0 × 1.9 × 4.5 mm and weighing 28.1 mg was sealed in a lead-glass capillary to avoid possible water loss during data collection. All data were collected using an Electronics-and-Alloys four-circle diffractometer at the CP-5 reactor and with the crystal mounted in a general orientation. The totally automated diffractometer is operated at the reactor or remotely (1 mile distant at the Chemistry Division) under the control of a Sigma V computer via a locally developed program package.[17] Neutrons diffracted from the (110) plane of a Be single crystal, at a monochromator angle of $\theta_m = 30°$, produce a monochromatic beam. The neutron flux at the sample position is ~2.9 × 10^6 N cm^{-2} s^{-1}.

Using the least-squares determined orientation matrix, data were automatically collected using the θ–2θ step-scan method with 0.1° step intervals and preset scan ranges of 40–55 steps. Background intensity measurements were obtained with the crystal and detector simultaneously stationary on both sides of each peak.

Two sets of intensity data (5037 reflections) were collected and averaged, the first to $2\theta = 110°$ (1380 independent reflections) but with c = 2.96 Å, and the second to $2\theta = 85°$ (3657 independent reflections) with the correct c = 11.83 Å. Averaging of all data[16] yielded 3969 independent reflections [3276 with $(F_o)^2 > \sigma(F_o)^2$] out to a maximum $\sin\theta/\lambda = 0.72$. Two reference reflections were remeasured after every 80 reflections in order to monitor instrument and crystal stability; their integrated intensities did not vary more than 3% during data collection. Each reflection was corrected for absorption (μ_c = 1.00 cm^{-1}). The minimum and maximum transmission coefficients were 0.838 and 0.892, respectively. Using the absorption corrected integrated intensities the F_o^2 were obtained by application of the following equation:[18] $F_o^2 = (wI \sin 2\theta)/(I_0\lambda^3N^2V)$, where I_0 is the incident intensity, λ the wavelength, w the angular velocity of rotation of the crystal, N the number of unit cells per unit volume, V the specimen volume, and θ the Bragg angle. A cylindrical NaCl crystal, for which precise absorption and secondary extinction corrections had been made for all reflections, was used to obtain I_0 and thereby place the F_o^2 on an approximate "absolute scale" whereby the starting scale factor (S) in the least-squares refinement is ~1.0. The variances of F_o^2 were calculated from $\sigma^2(F_o^2) = \sigma_c^2(F_o^2) + (0.03F_o^2)^2$, where $\sigma_c^2(F_o^2)$ is determined from the counting statistics and 0.03 is an added factor deduced from the 3% maximum variation in the integrated intensities of the reference reflections.

Table II. Final Discrepancy Indices

Data selection	No. of reflections	$R(F_o)$	$R(F_o^2)$	$R_w(F_o^2)$	σ_1[a]
All reflections	3969	0.077	0.077	0.082	1.45
$F_o^2 > \sigma(F_o^2)$	3276	0.056	0.073	0.081	1.58
Logic test[b]	3955	0.075	0.058	0.067	1.17
Logic test[b] and $F_o^2 > 1.0\sigma(F_o^2)$	3262	0.053	0.054	0.065	1.27

[a] See text for explanation of σ_1. [b] Data were excluded from the least-squares refinement if the transmission due to extinction was less than 40%.

Structure Solution and Refinement.[16] The structure was solved using the neutron Patterson map from which the positions of the $Pt(CN)_4^{-1.75}$ groups were derived. It was obvious that adjacent $Pt(CN)_4^{-1.75}$ groups were stacked along c with a ~45° staggered configuration of these groups. A full-matrix least-squares refinement of the Pt, C, and N positional parameters (with isotropic thermal parameters) yielded the following discrepancy indices:

$$R(F_o) = \frac{\Sigma ||F_o| - |F_c||}{\Sigma |F_o|} = 0.40$$

$$R(F_o^2) = \frac{\Sigma |F_o^2 - F_c^2|}{\Sigma F_o^2} = 0.48$$

and

$$R_w(F_o^2) = \left(\frac{\Sigma w_i |F_o^2 - F_c^2|^2}{\Sigma w_i F_o^4} \right)^{1/2} = 0.55$$

using all data. Fourier and difference Fourier maps were then calculated and all nonhydrogen atoms were located. An additional three cycles of least-squares refinement including Pt, C, and N atoms (anisotropic thermal parameters) and K and O atoms (isotropic thermal parameters) yielded $R(F_o) = 0.20$, $R(F_o)^2 = 0.24$, and $R_w(F_o^2) = 0.29$. At this stage all hydrogen atoms were located from a difference density map. An additional four cycles of least-squares refinement including $3Pt(CN)_4$, $3H_2O$, and $4K^+$ with anisotropic temperature factors and all atoms at full occupancy yielded $R(F_o) = 0.081$, $R(F_o)^2 = 0.080$, and $R_w(F_o)^2 = 0.085$. It was apparent at this point that an extinction correction was necessary and refinement was continued including an isotropic extinction parameter.[19] In the final refinement 14 observations were rejected due to severe extinction (transmission factors <0.6). At this stage the residual density maps were virtually featureless except for areas around K(4) and O(11); thermal ellipsoids[16] for these atoms were unusually elongated and in addition the calculated K–O distances were unexpectedly short being less than the van der Waals sum of ~2.7 Å. This suggested the presence of a K^+ and H_2O disorder and when full-matrix least-squares refinement was continued, convergence occurred with partial occupancy factors fixed [50% for K^+ due to the presence of a center of symmetry relating the two sites] for the K(4), O(11), and O(12) sites. The resulting K–O [K(4)–O(11); K(4)′–O(12)] distances are much more chemically reasonable as is discussed below. The final refinement with an isotropic extinction correction and anisotropic thermal parameters converged yielding the agreement factors given in Table II. The final change-to-esd ratio was less than 0.03 for all parameters except for the disordered atoms where the ratio was expectedly higher at 0.5. The standard deviation of an observation of unit weight

$$\sigma_1 = \left[\frac{w_i |F_o^2 - F_c^2|^2}{(n-p)} \right]^{1/2}$$

where n is the number of observations and p the number of parameters, varied (viz., 297) in the least-squares refinement, was 1.46 for all the data and the ratio of observations to parameters is ca. 14:1. Additional confirmation that the correct space group is $P\bar{1}$ was obtained using statistical intensity tests in the program MULTAN[16] which clearly indicated the structure to be centrosymmetric as follows:

	Exptl	Theor Centric	Theor Acentric
E^2	0.9995	1.0000	1.0000
MOD($E^2 - 1$)	1.0240	0.9680	0.7360
MOD(E)	0.7725	0.7980	0.8860

The final positional and thermal parameters are given in Table III and the important bond distances and angles in $K_{1.75}[Pt(CN)_4]\cdot 1.5H_2O$ are given in Table IV. For the least-squares refinement, the coherent neutron scattering amplitudes used for Pt, N, C, O, K, and H were respectively 0.950, 0.940, 0.665, 0.580, 0.370, and −0.374 all in units of 10^{-12} cm.[20]

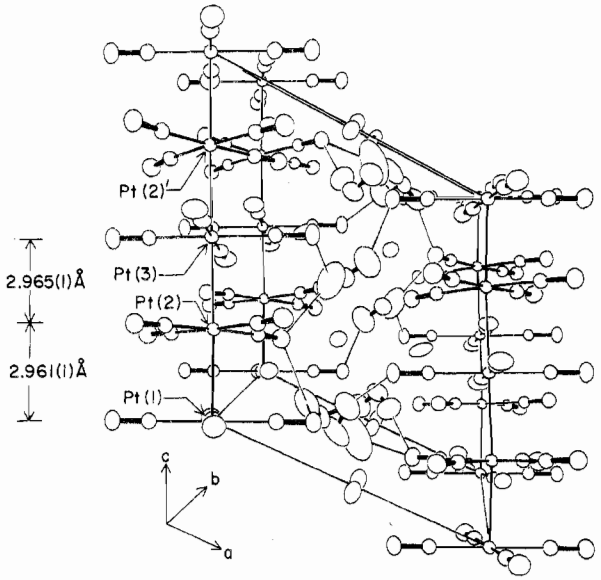

Figure 1. The unit cell drawing of $K_{1.75}[Pt(CN)_4]\cdot 1.5H_2O$ showing the nonlinear Pt(1)–Pt(2)–Pt(3) chain which extends along c and has equal Pt–Pt separations [bond angle 173.25 (3)°]. Thermal ellipsoids are scaled to enclose 50% probability. Inversion centers occur at Pt(1) and Pt(3) only. The Pt(2) atom is displaced 0.170 Å perpendicular to the c axis. Hydrogen bonds from H_2O to cyanide group nitrogen atoms (N···H < 2.6 Å) are indicated by faint lines and K^+ ions are shown without bonding interactions.

Structure Description

The Zig-Zag Pt Atom Chain. The structure basically comprises $Pt(CN)_4^{-1.75}$ groups which stack along the triclinic c axis to form an unusual quasi-one-dimensional Pt atom chain. These stacks are bound by both water molecules and K^+ ions indicating the main binding forces involve K^+ to $^-N{\equiv}C$ electrostatic attraction and dipolar $H_2O\cdots{}^-N{\equiv}C$ interactions. The interactions of K^+ with the cyanide nitrogen atoms of the platinocyanide groups appear to be the driving force for deformation of the Pt atom chain and will be discussed in detail shortly.

The asymmetric unit of the crystal contains three crystallographically independent $Pt(CN)_4^{-1.75}$ groups, four K^+ ions (one in disorder), and three H_2O molecules (one in disorder) and the unit cell is illustrated in Figure 1. The most significant and unusual finding is a nonlinear Pt atom chain as illustrated in the stereodiagram of the unit cell in Figure 2. The zig-zag Pt atom chain comprises Pt(1), Pt(2), and Pt(3) [bond angle 173.25 (3)°] which extends along c. The Pt(2) is on a general position with $z = 0.2568$ (1) and is displaced perpendicular to the c axis (on which the other two Pt atoms reside) by 0.170 (1) Å. The displacement is toward surrounding K^+ ions and away from the coordinated H_2O molecules. Inversion centers occur at Pt(1) and Pt(3) and therefore what might be considered to be the basic repeat unit of the chain is a linear

Table III. Positional and Thermal Parameters for $K_{1.75}[Pt(CN)_4]\cdot 1.5H_2O$ and Root-Mean-Square Thermal Displacements (in Å) of Atoms along Their Principal Ellipsoidal Axes[a,b]

	10^4x	10^4y	10^4z	$10^4\beta_{11}$	$10^4\beta_{22}$	$10^4\beta_{33}$	$10^4\beta_{12}$	$10^4\beta_{13}$	$10^4\beta_{23}$	$10^3\mu_1$	$10^3\mu_2$	$10^3\mu_3$
Pt(1)	0	0	0	53 (2)	52 (2)	35 (1)	−25 (1)	19 (1)	−14 (1)	129 (2)	131 (3)	149 (2)
Pt(2)	93 (1)	−211	2568 (1)	48 (1)	50 (1)	30 (1)	−20 (1)	16 (1)	−13 (1)	122 (2)	133 (2)	143 (1)
Pt(3)	0	0	5000	49 (2)	47 (2)	31 (1)	−16 (1)	18 (1)	−13 (1)	123 (2)	129 (2)	144 (2)
C(11)	2308 (2)	−621 (2)	930 (2)	67 (2)	83 (2)	55 (2)	−37 (2)	30 (1)	−28 (1)	150 (2)	169 (2)	170 (2)
C(12)	513 (2)	−2368 (2)	523 (2)	79 (2)	55 (2)	51 (2)	−32 (1)	32 (1)	−17 (1)	131 (2)	162 (2)	173 (2)
C(21)	−1202 (2)	−1477 (2)	2317 (2)	66 (2)	69 (2)	47 (1)	−35 (1)	27 (1)	−21 (1)	141 (2)	152 (2)	166 (2)
C(22)	1991 (2)	−2337 (2)	3658 (2)	61 (2)	63 (2)	44 (1)	−15 (1)	22 (1)	−13 (1)	138 (2)	159 (2)	170 (2)
C(23)	1388 (2)	1064 (2)	2771 (2)	68 (2)	76 (2)	51 (2)	−38 (1)	27 (1)	−26 (1)	142 (2)	162 (2)	170 (2)
C(24)	−1856 (2)	1836 (2)	1514 (1)	60 (2)	64 (2)	42 (1)	−16 (1)	20 (1)	−11 (1)	135 (2)	162 (2)	167 (2)
C(31)	−2315 (2)	754 (2)	4032 (2)	53 (2)	83 (2)	44 (2)	−20 (1)	19 (1)	−18 (1)	137 (2)	162 (2)	178 (2)
C(32)	−201 (2)	2276 (2)	4432 (2)	88 (2)	59 (2)	43 (1)	−28 (1)	32 (1)	−19 (1)	141 (2)	145 (2)	184 (2)
N(11)	3652 (1)	−1030 (2)	1471 (1)	71 (2)	162 (2)	81 (2)	−52 (1)	33 (1)	−42 (1)	155 (2)	211 (2)	239 (2)
N(12)	879 (1)	−3753 (1)	844 (1)	127 (2)	62 (1)	83 (1)	−42 (1)	54 (1)	−24 (1)	140 (2)	206 (2)	219 (1)
N(21)	−1958 (1)	−2205 (1)	2154 (1)	98 (1)	102 (2)	72 (1)	−64 (1)	42 (1)	−34 (1)	149 (2)	190 (2)	208 (1)
N(22)	3018 (1)	−3610 (1)	4301 (1)	87 (1)	80 (1)	67 (1)	−3 (1)	28 (1)	−14 (1)	146 (2)	198 (2)	224 (1)
N(23)	2077 (1)	1861 (2)	2820 (1)	112 (2)	132 (2)	88 (2)	−86 (1)	47 (1)	−46 (1)	148 (2)	212 (2)	235 (2)
N(24)	−2996 (1)	3022 (1)	924 (1)	81 (1)	94 (2)	76 (1)	1 (1)	30 (1)	−6 (1)	146 (2)	210 (2)	239 (2)
N(31)	−3658 (1)	1172 (2)	3478 (1)	56 (1)	159 (2)	83 (2)	−30 (1)	23 (1)	−38 (1)	143 (2)	222 (2)	245 (2)
N(32)	−267 (2)	3570 (1)	4106 (1)	168 (2)	69 (1)	75 (1)	−58 (1)	65 (1)	−27 (1)	142 (2)	187 (2)	252 (1)
K(1)	3999 (3)	3952 (4)	3293 (3)	101 (4)	138 (4)	79 (3)	−20 (3)	46 (3)	−38 (3)	177 (4)	198 (4)	249 (4)
K(2)	−2717 (5)	−3853 (4)	3918 (4)	229 (6)	163 (5)	124 (5)	−114 (5)	136 (5)	−81 (4)	167 (5)	212 (4)	300 (4)
K(3)	−1121 (3)	5011 (3)	1294 (3)	121 (4)	98 (4)	68 (3)	−55 (3)	48 (3)	−30 (3)	172 (4)	185 (4)	214 (3)
K(4)[c]	5079 (18)	265 (16)	139 (16)	80 (9)	177 (25)	85 (13)	−16 (12)	43 (10)	6 (10)	167 (6)	188 (8)	304 (16)
O(11)[c]	3512 (6)	2525 (7)	969 (7)	100 (6)	117 (6)	71 (6)	−83 (6)	17 (5)	18 (4)	96 (11)	170 (7)	300 (7)
O(12)[c]	4031 (14)	2475 (13)	737 (12)	248 (22)	245 (14)	109 (11)	−136 (17)	−10 (12)	−13 (9)	202 (11)	264 (11)	417 (16)
O(2)	5474 (3)	5189 (3)	1997 (2)	151 (3)	134 (3)	78 (3)	−19 (3)	38 (3)	−25 (2)	190 (3)	222 (3)	282 (3)
O(3)	4476 (3)	1694 (3)	5506 (3)	132 (3)	140 (3)	91 (3)	−61 (3)	46 (2)	−40 (2)	208 (3)	217 (3)	240 (3)
H(11,1)[c]	4524 (8)	2084 (7)	1706 (7)	192 (9)	225 (8)	141 (9)	−55 (7)	31 (8)	−54 (7)	236 (8)	289 (6)	346 (7)
H(11,2)[c]	3020 (10)	1954 (11)	1272 (8)	230 (14)	272 (16)	101 (9)	−214 (14)	34 (9)	45 (10)	53 (24)	230 (9)	441 (12)
H(12,2)[c]	4786 (31)	2682 (41)	776 (40)	333 (51)	621 (86)	408 (70)	−98 (46)	−23 (46)	−254 (64)	305 (24)	416 (29)	652 (46)
H(21)	4659 (6)	5945 (6)	1140 (5)	189 (7)	226 (8)	114 (6)	−55 (6)	51 (6)	8 (6)	211 (6)	287 (5)	342 (6)
H(22)	5997 (6)	4351 (6)	1795 (5)	209 (7)	206 (7)	172 (7)	−81 (6)	115 (6)	−98 (6)	230 (6)	281 (5)	297 (6)
H(31)	5391 (7)	1121 (7)	6342 (7)	212 (9)	281 (11)	150 (8)	−53 (8)	30 (7)	13 (7)	228 (6)	337 (6)	391 (8)
H(32)	4044 (7)	988 (7)	5296 (8)	266 (10)	284 (10)	375 (15)	−186 (9)	205 (10)	−230 (11)	222 (6)	280 (6)	440 (8)

[a] The estimated standard deviations in parentheses for this and all subsequent tables refer to the least-significant figure. [b] The form of the temperature factor is $\exp\{-(\beta_{11}h^2 + \beta_{22}k^2 + \beta_{33}l^2 + 2\beta_{12}hk + 2\beta_{13}hl + 2\beta_{23}kl)\}$. [c] Atoms in crystallographic disorder and multipliers were adjusted appropriately for partial occupancy.

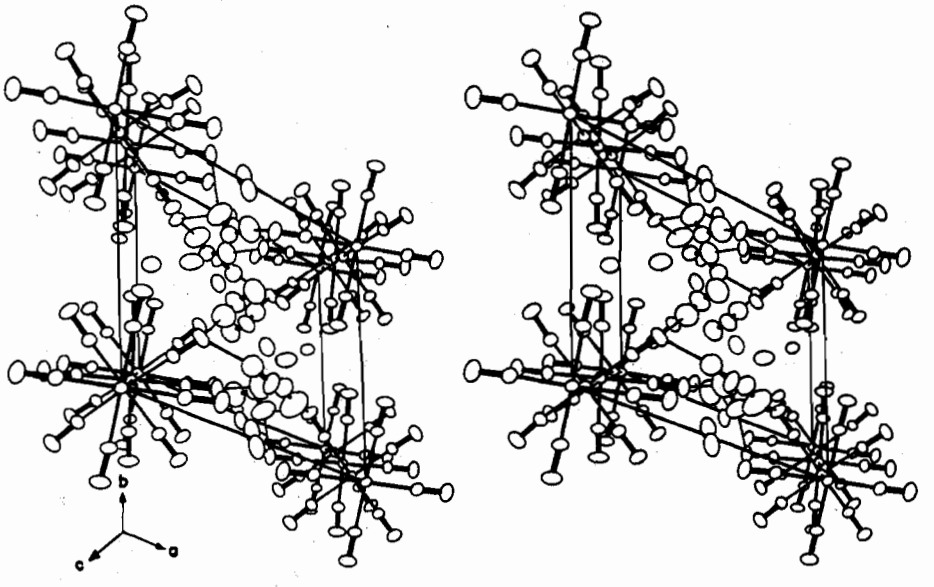

Figure 2. Stereodrawing of the structure of triclinic $K_{1.75}[Pt(CN)_4]\cdot 1.5H_2O$ which clearly illustrates both the "zig-zag" nature of the Pt atom chain and the molecular packing. One of the four K^+ (at ~0.5,0,0) is involved in disorder with one of the three H_2O molecules [O(11) and O(12), see Table III for coordinates].

three-atom array [Pt(2)′–Pt(1)–Pt(2) or alternatively Pt-(2)–Pt(3)–Pt(2)′] where the bond angle [173.25 (3)°] between the three atom subunits indicates significant nonlinearity. However, the surprising finding (see Figure 1) is that the two crystallographically *independent* Pt–Pt bond lengths are of *equal* length [2.961 (1) and 2.965 (1) Å] and yet they exceed the distance in Pt metal (~2.78 Å) by approximately 0.18 Å. The implications of the equality of the Pt–Pt separations are discussed below.

The $Pt(CN)_4$ Groups. The $Pt(1)(CN)_4^{-1.75}$ and $Pt(3)(CN)_4^{-1.75}$ groups, associated with Pt atoms at centers of symmetry, are nearly planar as shown in Table V in which the best least-squares planes for these groups are presented. However, it is quite clear from Table V that the Pt(2) pla-

Table IV. Interatomic Distances (Å) and Bond Angles (deg) for $K_{1.75}[Pt(CN)_4]\cdot 1.5H_2O$[a]

(A) Distances around Platinum Atoms

Pt(1)-Pt(2)	2.961 (1)	Pt(2)-Pt(3)	2.965 (1)
Pt(1)-C(11)	2.002 (1)	Pt(2)-C(21)	1.996 (2)
Pt(1)-C(12)	1.999 (1)	Pt(2)-C(22)	2.008 (2)
Pt(3)-C(31)	1.991 (1)	Pt(2)-C(23)	2.004 (2)
Pt(3)-C(32)	2.000 (1)	Pt(2)-C(24)	1.991 (2)
(Pt-C) Av 1.999 (4)			

(B) Carbon-Nitrogen Distances in Cyanide Groups

C(11)-N(11)	1.159 (2)	C(21)-N(21)	1.156 (2)
C(12)-N(12)	1.158 (2)	C(22)-N(22)	1.157 (2)
C(31)-N(31)	1.157 (2)	C(23)-N(23)	1.160 (2)
C(32)-N(32)	1.155 (2)	C(24)-N(24)	1.159 (2)
(C-N) Av 1.158 (6)			

(C) Potassium Ion Interactions

K(1)-O(3)	2.734 (4)	K(2)-O(3)	2.718 (4)
K(1)-O(2)	2.864 (4)	K(2)-O(2)	2.779 (4)
K(1)-N(31)	2.899 (3)	K(2)-N(21)	2.828 (3)
K(1)-N(22)	2.912 (3)	K(2)-N(32)	2.847 (4)
K(1)-N(12)	3.002 (3)	K(2)-N(22)	2.987 (3)
K(1)-N(22)′	3.074 (3)		
K(3)-O(11)	2.677 (7)	K(4)[b]-N(11)	2.81 (2)
K(3)-O(12)	2.807 (11)	K(4)-N(21)	2.82 (2)
K(3)-N(12)	2.811 (3)	K(4)-N(11)	2.87 (2)
K(3)-N(32)	2.932 (3)	K(4)-O(11)	2.88 (2)
K(3)-N(24)	3.009 (3)	K(4)-N(21)′	2.89 (2)
K(3)-N(21)	3.018 (3)	K(4)-N(21)″	3.01 (2)
K(3)-H(11,12)	3.040 (8)		
K(3)-N(12)	3.077 (3)		

(D) Water Molecule O-H Bond Distances

O(11)[b]-H(11,1)	0.931 (9)	O(2)-H(21)	0.937 (6)
O(11)[b]-H(11,2)[b]	0.945 (7)	O(2)-H(22)	0.953 (6)
O(12)[b]-H(11,1)	0.97 (2)	O(3)-H(31)	0.930 (7)
O(12)[b]-H(12,2)[b]	0.84 (4)	O(3)-H(32)	0.915 (6)

(E) Interatomic Distances and Angles Involving Hydrogen Atoms

O(11)[b]-N(31)	2.832 (6)	O(11)[b]-H(11,1)-N(31)	165.5 (7)
H(11,1)-N(31)	1.921 (7)		
O(11)[b]-N(23)	3.169 (6)	O(11)[b]-H(11,2)[b]-N(23)	137 (1)
H(11,2)[b]-N(23)	2.41 (1)		
O(11)[b]-N(11)	3.181 (6)	O(11)[b]-H(11,2)[b]-N(11)	120 (1)
H(11,2)[b]-N(11)	2.60 (1)		
O(12)[b]-N(24)[c]	3.18 (1)	O(12)[b]-H(12,2)[b]-N(24)[c]	175 (3)
H(12,2)[b]-N(24)[c]	2.34 (4)		
O(2)-N(24)[d]	3.000 (3)	O(2)-H(21)-N(24)[d]	161.6 (5)
H(21)-N(24)[d]	2.096 (5)		
O(2)-N(24)[c]	3.028 (3)	O(2)-H(22)-N(24)[c]	165.0 (4)
H(22)-N(24)[c]	2.098 (5)		
O(3)-N(11)[e]	3.083 (3)	O(3)-H(31)-N(11)[e]	138.6 (6)
H(31)-N(11)[e]	2.324 (8)		
O(3)-N(31)[f]	3.164 (3)	O(3)-H(32)-N(31)[f]	135.5 (7)
H(32)-N(31)[f]	2.446 (6)		
O(3)-N(23)[g]	3.496 (3)	O(3)-H(32)-N(23)	115.3 (6)
H(32)-N(23)	2.538 (8)		

(F) Angles within the Platinum Cyanide Groups

Pt(1)-C(11)-N(11)	177.8 (1)	Pt(2)-C(23)-N(23)	176.4 (1)
Pt(1)-C(12)-N(12)	176.9 (1)	Pt(2)-C(24)-N(24)	178.5 (1)
C(11)-Pt(1)-C(12)	87.25 (5)	C(21)-Pt(2)-C(22)	87.56 (6)
Pt(3)-C(31)-N(31)	179.1 (1)	C(21)-Pt(2)-C(23)	178.4 (1)
Pt(3)-C(32)-N(32)	177.6 (1)	C(21)-Pt(2)-C(24)	89.58 (7)
C(31)-Pt(3)-C(32)	91.65 (6)	C(22)-Pt(2)-C(23)	92.60 (7)
Pt(2)-C(21)-N(21)	179.1 (1)	C(22)-Pt(2)-C(24)	176.82 (8)
Pt(2)-C(22)-N(22)	175.2 (1)	C(23)-Pt(2)-C(24)	90.29 (6)

(G) Angles within the Water Molecules

H(11,1)-O(11)[b]-H(11,2)[b]	103.4 (8)	H(21)-O(2)-H(22)	102.4 (5)
H(11,1)-O(12)[b]-H(12,2)[b]	91 (3)	H(31)-O(3)-H(32)	107.5 (6)

[a] All distances are uncorrected for thermal motion. [b] This atom is in crystallographic disorder and only the chemically reasonable interatomic distances are given (see text and Figure 4). [c] Transformed by $(1 + x, y, z)$. [d] Transformed by $(\bar{x}, 1 - y, \bar{z})$. [e] Transformed by $(1 - x, \bar{y}, 1 - z)$. [f] Transformed by $(\bar{x}, \bar{y}, 1 - z)$. [g] Transformed by $(1 - x, \bar{y}, 1 - z)$.

Table V. Equations of "Best" Least-Squares Planes for the $Pt(CN)_4^{-1.75}$ Groups, Perpendicular Distances (Å) from These Planes, and Dihedral Angles between Normals of Planes[a-c]

(A) Plane I through Pt(1), C(11), C(12), N(11), and N(12)
$-4.294x + 1.652y + 11.821z - 0.003 = 0.0$

Pt(1)	−0.003 (1)	N(11)	−0.002 (2)
C(11)	0.004 (2)	N(12)	−0.003 (2)
C(12)	0.004 (2)		

(B) Plane II through Pt(2), C(21), C(22), C(23), C(24), N(21), N(22), N(23), and N(24)
$-4.194x + 2.218y + 11.828z - 2.950 = 0.0$

Pt(2)	0.002 (2)	N(21)	−0.071 (2)
C(21)	−0.033 (2)	N(22)	0.071 (2)
C(22)	0.024 (2)	N(23)	−0.073 (2)
C(23)	−0.019 (2)	N(24)	0.071 (2)
C(24)	0.028 (2)		

(C) Plane III through Pt(3), C(31), C(32), N(31), and N(32)
$-4.076x + 2.640y + 11.802z - 5.904 = 0.0$

Pt(3)	−0.003 (1)	N(31)	0.002 (2)
C(31)	−0.003 (2)	N(32)	−0.007 (2)
C(32)	0.011 (2)		

Dihedral Angles (deg) between Normals of Planes

I and II	3.7	I and *ab*	31.0
I and III	6.4	I and *ac*	87.5
II and III	2.7	I and *bc*	88.8
II and *ab*	33.2	III and *ab*	34.7
II and *ac*	88.8	III and *ac*	86.2
II and *bc*	89.7	III and *bc*	89.7

[a] The equations of the planes are expressed in the triclinic fractional coordinates x, y, z. [b] The atomic positions used in the calculation of a given plane were weighted according to the errors in the fractional coordinates. [c] The sense of the distances given is that + corresponds to the $+\vec{c}$.

tinocyanide group is significantly nonplanar.

The platinocyanide groups possess Pt–C bond distances which are all within 2σ of the average [1.999 (4) Å] and therefore these distances are essentially identical (Table IVA). The C≡N distances are identical to within $\sigma/2$ of the average value [1.158 (6) Å] (Table IVB). While the platinocyanide group Pt–C and C≡N distances are identical, within the errors of the measurements, the C–Pt–C bond angles all differ significantly from 90°; therefore, the platinocyanide groups are not strictly square but are nearly planar in the case of Pt(1) and Pt(3) only. The torsion angles between the platinocyanide groups, which is an indication of the degree of Pt($5d_{z^2}$) orbital overlap and cyanide group repulsion between *adjacent* groups in the stacks, are presented in Figure 3.[14] These angles between adjacent groups are all significantly different from 45° and have ranges as follows: Pt(1)–Pt(2), 41.3–46.4° and Pt(2)–Pt(3), 38.5–51.8°. Symmetry requirements are such that Pt(1) and Pt(3) must have symmetric ($\bar{1}$) crystalline environments, while Pt(2), which resides at a site with no symmetry restrictions, possesses a very *asymmetric* crystalline environment. The effect of the asymmetric crystalline environment about Pt(2) is to distort the Pt–Pt chain in a most predictable manner as discussed in a later section.

The K^+–H_2O Disorder and Hydrogen Bonding in $K_{1.75}[Pt(CN)_4]\cdot 1.5H_2O$. As indicated in Table IVC the primary coordination sphere of all K^+ ions [K(1)–K(4)] involves interactions of two types only, viz., $K^+\cdots OH_2$ or $K^+\cdots{}^-N{\equiv}C$. In both *anion* deficient compounds $K_2[Pt(CN)_4]X_{0.3}\cdot 3H_2O$, $X = Br^-$ or Cl^-, we observed disordered halide ions.[3,4] We have now found one K^+ and one H_2O molecule [K(4) and O(11)–O(12)], respectively, are disordered in the case of K(def)TCP. The potassium ion is disordered by a slight displacement from a center of inversion at $(1/2,0,0)$ as illustrated in Figure 4. The result is two positions with 0.80 (2) Å separation and with overall occupancy factors of 50% as required by the inversion center. It should be pointed out that the K^+ disorder requires a single unit cell to be non-

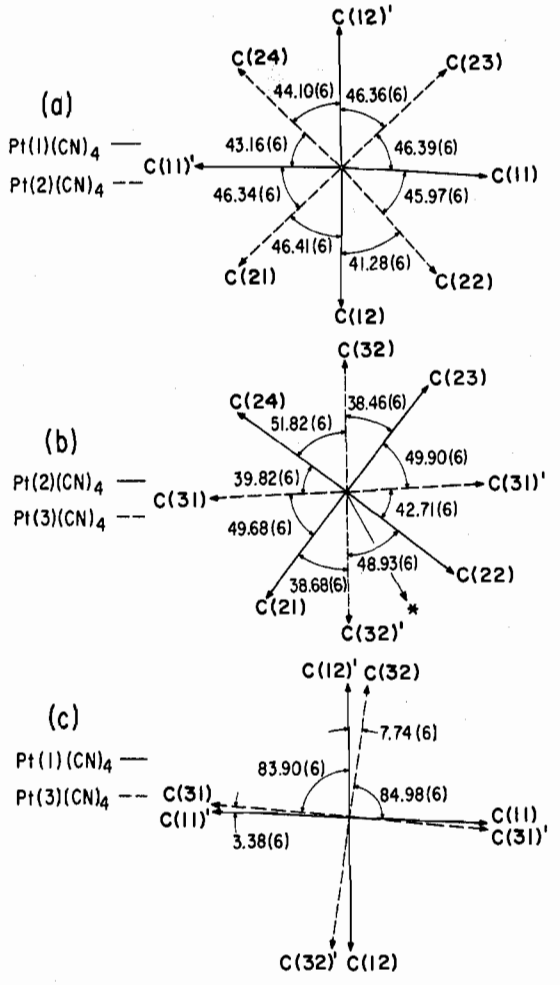

Figure 3. Torsion angles between the three independent platinocyanide groups in $K_{1.75}[Pt(CN)_4]\cdot 1.5H_2O$. The direction in which Pt(2) is displaced is indicated with an →*.

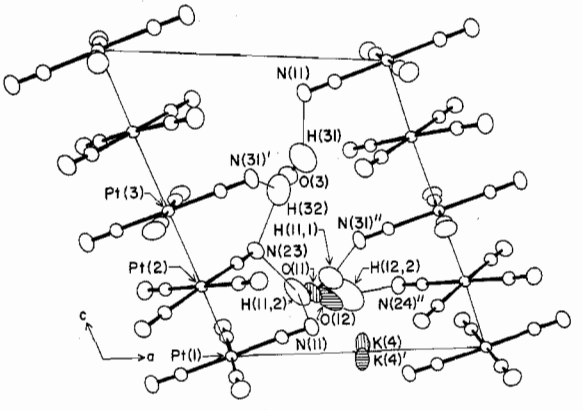

Figure 4. View of the *ac* section showing the hydrogen bonding, the $K^+\cdots H_2O$ disorder, and the site occupancy correlations. Water molecule to cyanide nitrogen atom hydrogen bonds (H···N < 2.6 Å) are indicated by faint lines. The outline of the *ac* section is also shown as faint lines. The occupancy code is as follows: when the vertically lined potassium site [K(4)] is occupied then the vertically lined oxygen site [O(11)] is also occupied. The same scheme applies to the horizontally lined positions. Note H(11,2) and H(12,2) have the same occupancy factors as O(11) and O(12) [see text].

centrosymmetric; however, the overall K^+ distribution in the crystal is centrosymmetric.

The disordered oxygen atoms [O(11) and O(12)] are not related by symmetry. However, the oxygen atom occupancy factors were restricted to equal those for K(4), since if the water disorder were not correlated to the K(4) disorder, chemically unreasonable K–O distances much less than the sum of the van der Waals radii (~2.7 Å) would result. Only one of the hydrogen atoms of the disordered water molecule is disordered as shown in Figure 4. The occupancies of its two sites, H(11,2) and H(12,2), were restricted to be equal to their corresponding oxygen occupancies (i.e., 50%). The other hydrogen atom, H(11,1), is not disordered and forms the shortest N···H distance (1.9 Å) in the structure. The H_2O molecule appears to pivot about the H(11,1)–N(31)″ vector axis, and in one of its "pivotal" positions it links adjacent $Pt(CN)_4^{-1.75}$ groups within a chain. In its alternate position it cross-links groups on different chains. Figure 4 shows the overall hydrogen bonding in the *a–c* section in addition to the occupancy correlation of the disordered K^+ ion and water molecule. Water molecule $H_2O(2)$ binds platinocyanide groups in *non*-adjacent stacks as shown in Figure 5.

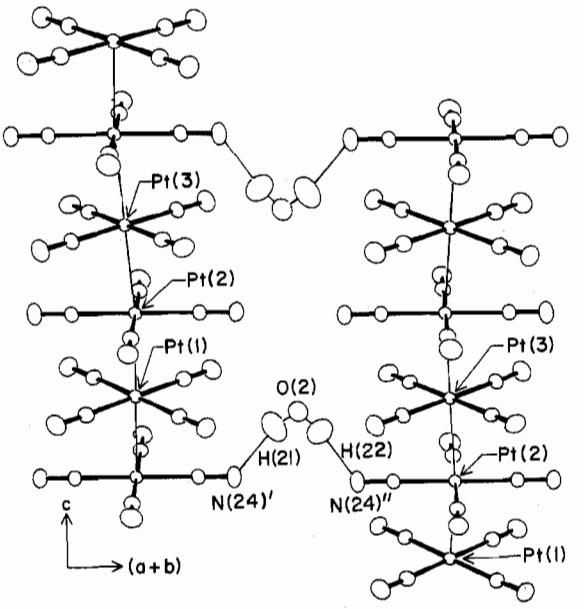

Figure 5. View of the {110} section showing both the interchain platinocyanide group linking by $H_2O(2)$ and the Pt chain distortion. Hydrogen bonds are drawn as faint lines.

The Pt Chain Deformation Resulting from an Asymmetric Crystalline Environment about Pt(2). As noted above, Pt(1) and Pt(3) reside at centers of symmetry and are therefore constrained to *centrosymmetric* ($\bar{1}$) crystalline environments. However, Pt(2) possesses a very acentric environment. About the $Pt(2)(CN)_4^{-1.75}$ group, the structure comprises largely H_2O on one side (+*b* side) and K^+ ions on the other (–*b* direction) as illustrated stereoscopically in Figure 6. This is illustrated graphically in Figure 7 in which all cyanide N atom coordination (out to 3.2 Å) is given.

The cause of the Pt chain distortion is readily apparent from Figures 6 and 7. In the direction of the Pt chain distortion (–*b* direction), the cyanide nitrogen atoms have a total of *six* K^+ nearest neighbors while in the +*b* direction there are only *two* K^+ to CN^- interactions in addition to weak hydrogen bonding interactions. Thus the distortion of the chain is clearly due to the unbalanced $K^+\cdots{}^-N{\equiv}C$ coulombic interactions of the $Pt(2)(CN)_4^{-1.75}$ group.

Structural Comparisons of $K_{1.75}[Pt(CN)_4]\cdot 1.5H_2O$, $K_2[Pt(CN)_4]Br_{0.3}\cdot 3H_2O$, and $K_2[Pt(CN)_4]\cdot 3H_2O$. For the later purpose of understanding the crystal structure modifications required to produce short Pt–Pt separations and linear chains in these cation deficient compounds, it is informative to compare the structural perturbations of $M^+\cdots{}^-N{\equiv}C$ interactions on the Pt–Pt chains in *unoxidized* $K_2[Pt(CN)_4]\cdot 3H_2O$[7] (Figure 8a) and the *partially oxidized* platinocyanides

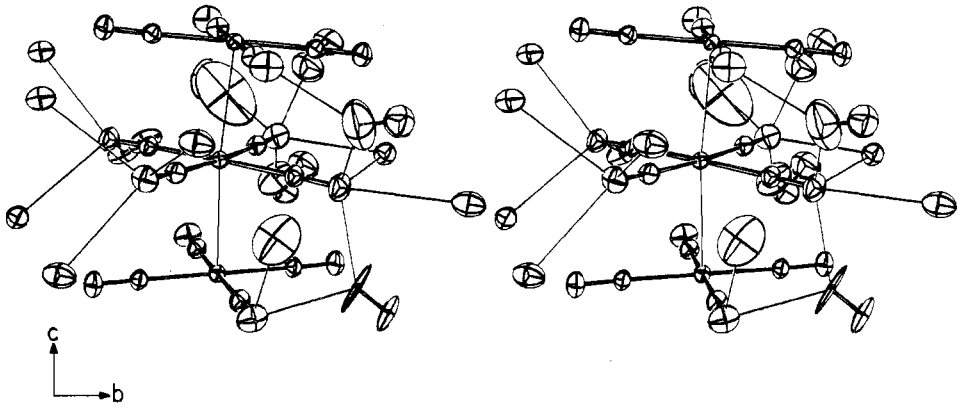

Figure 6. Stereodiagram of the asymmetric crystalline environment about Pt(2). All Pt(2) cyanide nitrogen atom neighbors to 3.2 Å are included in addition to a 5 Å coordination sphere about Pt(2). Atom labeling is shown in Figure 7.

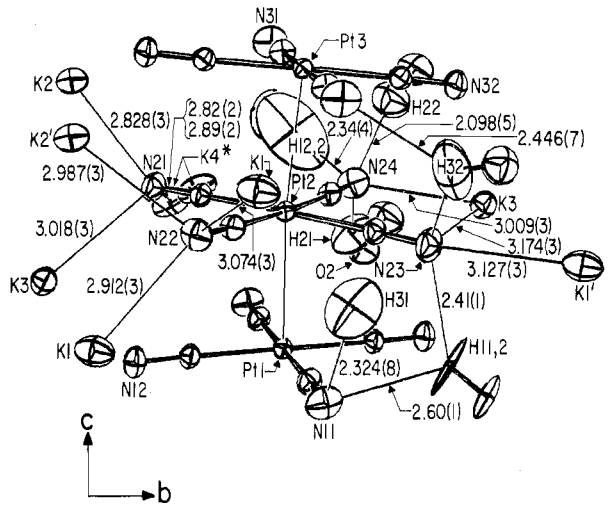

Figure 7. Diagram showing atom labels and bond distances for the coordination spheres of Pt(2) and its cyanide nitrogens. The transverse Pt chain distortion is in the $-b$ direction as would be expected due to the unbalanced $K^+ \cdots {}^-N{\equiv}C$ Coulombic interactions (a total of six in the $-b$ direction and only two in $+b$). Only interactions to Pt(2) nitrogens are indicated since symmetry inversion centers at Pt(1) and Pt(3) prohibit any transverse displacement of these atoms.

$K_2[Pt(CN)_4]Br_{0.3}\cdot 3H_2O$[3] (Figure 8b) and $K_{1.75}[Pt(CN)_4]\cdot 1.5H_2O$ (Figure 7). At this point it is also useful to introduce the concept of the "degree of partial oxidation", DPO, of the Pt metal atom assuming it to be 0.0 in unoxidized $K_2[Pt(CN)_4]\cdot 3H_2O$. The DPO is 0.30 in $K_2[Pt(CN)_4]\cdot Br_{0.3}\cdot 3H_2O$ (0.33 if the Br^- content is considered as 0.33)[3] and 0.25 in $K_{1.75}[Pt(CN)_4]\cdot 1.5H_2O$. We naturally expect that in the partially oxidized complexes if no other forces prevail the Pt–Pt separations will increase as the DPO decreases. Two forces which influence the structures of these materials, in addition to the DPO, are: (i) the strength *and number* of $M^+ \cdots {}^-N{\equiv}C$ interactions formed (sometimes chain "distorting" and sometimes chain "compressing" vide infra) and (ii) the degree of CN^- π–π cloud repulsion between adjacent $Pt(CN)_4$ groups. Both (i) and (ii) appear to be intimately related in the partially oxidized complexes.

It is most illuminating to compare the structural effects of (i) and (ii), for Na^+ and K^+, in the specific case where the DPO = 0.0 and is not a contributing factor in determining the structure. For $K_2[Pt(CN)_4]\cdot 3H_2O$ and $NaK[Pt(CN)_4]\cdot 3H_2O$[21] although the DPO is zero the Pt–Pt separations and cyanide torsion angles are respectively 3.478 (1) Å and ~16° in the former and 3.25 Å and 36° in the latter. It seems clear that the substantial reduction in Pt–Pt bond length of ~0.23 Å in $NaK[Pt(CN)_4]\cdot 3H_2O$ is related only to the crystal

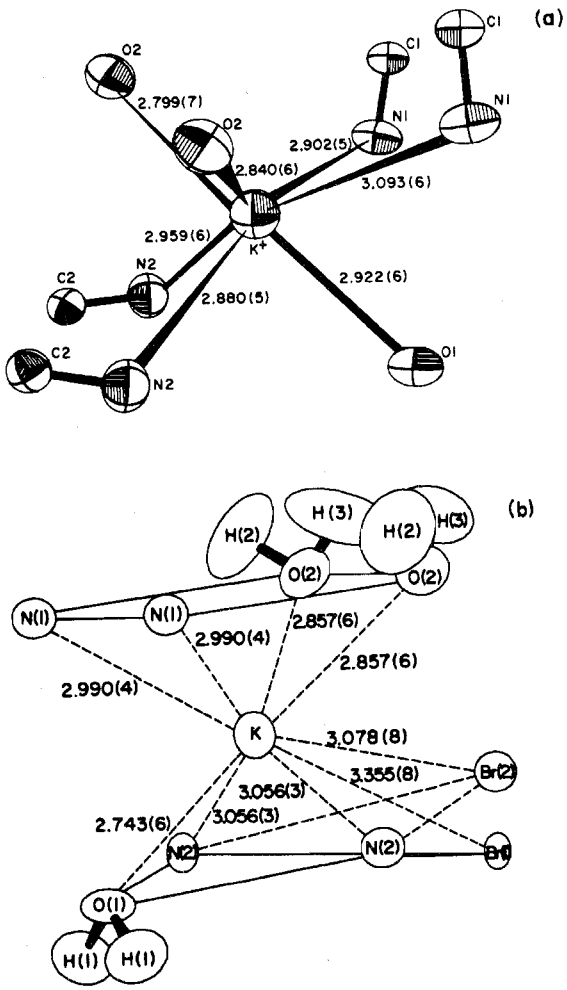

Figure 8. Composite diagram showing the potassium ion interactions in (a) $K_2[Pt(CN)_4]\cdot 3H_2O$, the unoxidized starting product, and (b) $K_2[Pt(CN)_4]Br_{0.3}\cdot 3H_2O$, the *anion* deficient analogue of $K_{1.75}[Pt(CN)_4]\cdot 1.5H_2O$. The Pt–Pt separations in $K_2[Pt(CN)_4]\cdot 3H_2O$ are long (3.48 Å) while in $K_2[Pt(CN)_4]Br_{0.3}\cdot 3H_2O$ they are much shorter (2.89 Å).

packing forces involving $Na^+ \cdots {}^-N{\equiv}C$ vs. $K^+ \cdots {}^-N{\equiv}C$ interactions. In $K_2[Pt(CN)_4]\cdot 3H_2O$[7] (Figure 8a) the $K^+ \cdots N$ distances all exceed the $K^+ \cdots N$ van der Waals sum (~2.8 Å) as is also the case in $NaK[Pt(CN)_4]\cdot 3H_2O$; however, in the latter, one-half of the $Na^+ \cdots N$ distances (2.39 Å) are *less* than the van der Waals sum (~2.5 Å) indicating that the $Pt(CN)_4^{2-}$ torsion angle of ~36° is caused by $Na^+ \cdots {}^-N{\equiv}C$ attractive interactions. Recently we have shown that even the relatively long $K^+ \cdots {}^-N{\equiv}C$ distances (2.99–3.06 Å) observed

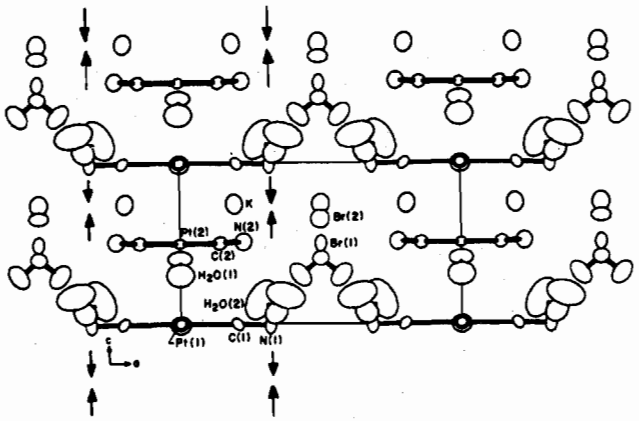

Figure 9. Diagram showing the longitudinal distortions of the Pt chain in $K_2[Pt(CN)_4]Br_{0.3}\cdot 3H_2O$ as caused by the $K^+\cdots{}^-N{\equiv}C$ interactions. Note that the *4mm* symmetry and alternating layers of K^+ ions dictate the directions in which the potassium ions compress the Pt chains.

in $K_2[Pt(CN)_4]Br_{0.3}\cdot 3H_2O$[3] (Figure 8b) are sufficient to cause the cyanide nitrogen atoms to "cant" toward K^+ as illustrated in Figure 9. Thus the distribution of the M^+ ion and the $M^+\cdots{}^-N{\equiv}C$ distances formed are extremely influential in determining both the Pt–Pt separations and chain structure in these compounds.

It is clear that the *acentric* K^+ distribution about Pt(2) causes the transverse Pt chain distortion observed in triclinic $K_{1.75}[Pt(CN)_4]\cdot 1.5H_2O$ (Figure 7). In the case of tetragonal $K_2[Pt(CN)_4]Br_{0.3}\cdot 3H_2O$, even though the Pt(1) and Pt(2) *environments* are noncentrosymmetric, *the K^+ ion placement* (equally distributed on each side of the Pt atoms as required by the *4mm* site symmetry; Figure 8) is such that the $K^+\cdots{}^-N{\equiv}C$ attractive forces tend only to "compress" Pt atom pairs in the chain and could thereby promote formation of two distinct Pt–Pt separations. Therefore, there is *no* tendency for the K^+ distribution in tetragonal KCP(Br) to cause transverse distortion of the chain. The anticipated effects on Pt chain deformation of varying the cation size and charge are discussed in the Conclusions and Predictions section.

One question that arises at this point is why the Pt–Pt separations in K(def)TCP are 0.069–0.077 Å longer than in KCP(Br). A most plausible and yet simple explanation is to be found when considering the relative *changes* in DPO of Pt in these two materials. Assuming the molar Br^- content of KCP(Br) to be 0.30–0.33, the Pt oxidation state is +2.30–2.33 while in K(def)TCP it is +2.25. Assuming, in this case, that there is a simple relationship between Pt valence state and Pt–Pt separation, then in the K(def)TCP the Pt–Pt separation should lengthen by a factor of 1.022–1.036 over that in KCP(Br) [2.89 (1) Å] leading to an expected separation of 2.95–2.99 Å. The observed Pt–Pt separation of 2.96 Å is in excellent agreement with this expectation. Although Krogmann has suggested that there "appears to be no strict relationship between Pt–Pt distance and the oxidation number",[22] it appears that within a specific group of partially oxidized chain-forming platino*cyanide* salts, of similar crystal structure, this linear relationship may hold. This relationship may fail for very short Pt–Pt separations where metal–metal repulsive forces become important. It is unlikely that these repulsive forces are important in these partially oxidized complexes because the Pt–Pt separations are ~0.1 Å greater than in Pt metal (2.78 Å) while in Pt metal cluster or alkyl systems the metal–metal separations are often shorter than those in the metal by as much as ~0.1–0.2 Å.[23a-d] It is worth pointing out that only unoxidized $K_2[Pt^{II}(CN)_4]\cdot 3H_2O$, and not the fully oxidized $K_2[Pt^{IV}(CN)_4]Br_2$,[24] may represent an extreme point in determining Pt–Pt bond distance vs. oxidation number because the latter compound possesses an entirely different crystal structure which does not contain Pt–Pt chains. We have pointed out elsewhere[23e] that the Pt–Pt separations in one-dimensional salts may also be calculated using Paulings'[32] theory of the metallic bond.

Polarized Specular Reflectance, Inelastic Neutron Scattering, and X-Ray Diffuse Scattering Studies of $K_{1.75}[Pt(CN)_4]\cdot 1.5H_2O$. It has been pointed out elsewhere[25] that polarized specular reflectance spectroscopy can be used to clearly distinguish between one-dimensional metal and semiconductor systems. Halide deficient $K_2[Pt(CN)_4]Br_{0.3}\cdot 3H_2O$ has been studied using this technique and strongly reflects (80–90%) photon energies less than 2.0 eV even in the FIR which confirms that KCP(Br) has metallic behavior parallel to the Pt–Pt chain.[25,26] We have made similar room-temperature measurements of $K_{1.75}[Pt(CN)_4]\cdot 1.5H_2O$ and find approximately 85–90% reflectivity parallel to the Pt–Pt chain and only 5–10% perpendicular to the chain.[27] Clearly K(def)TCP has 1-D metallic character at room temperature. Incomplete conductivity measurements of K(def)TCP have been published in which the conductivity is reportedly lower than in KCP(Br).[28] However, this merits reinvestigation now that the structure is well characterized.

Using inelastic neutron scattering techniques, we have observed evidence of strong electron–phonon coupling in K(def)TCP which also definitely indicates the metallic character of this salt.[29] This study has been made using hydrogenated samples and the work will be extended using deuterated single crystals.

Using photographic techniques, we have observed (room temperature) x-ray diffuse scattering from single crystals of K(def)TCP.[30] Using KCP(Br) crystals for calibration, we have confirmed the results of Comes et al.[31] in which diffuse satellite lines are observed about the intense layer lines. The derived superstructure repeat separation for K(def)TCP is, within experimental error, eight times the Pt–Pt separation (2.96 Å). Thus we observed a Kohn anomaly in K(def)TCP and the composition derived from the superstructure repeat separation is in excellent agreement with that expected for $K_{1.75}[Pt(CN)_4]\cdot 1.5H_2O$. Additional low-temperature studies are in progress.

Conclusions and Predictions

The crystal and molecular structure of $K_{1.75}[Pt(CN)_4]\cdot 1.5H_2O$ has been discussed in considerable detail in the previous sections. In both K(def)TCP and KCP(Br) the short Pt–Pt separations are due to increased d_{z^2} orbital overlap resulting from removal of electrons from Pt upon partial oxidation[22] and, based on the Pt–Pt separations only, it would appear that the metal–metal bond in K(def)TCP is clearly weaker than in KCP(Br). Actually we may calculate an approximate force constant k for the Pt–Pt bonds in these materials using the method suggested by Pauling[32] where $k^{-1/2} = a_{ij}(D_e - b_{ij})$; D_e is the equilibrium internuclear distance (2.96 Å), and a_{ij} and b_{ij} are constants derived for metals and metalloids.[32] The derived value for k is ~0.121 Mdyn/cm and from this we may calculate an approximate restoring force on Pt(2), which is displaced perpendicular to c by 0.170 Å, of 2.06×10^{-4} dyn. Utilizing this method of calculation one can predict that for K(def)TCP and KCP(Br) the Pt–Pt vibration should occur at approximately 140–160 cm^{-1}. We have reported vibrational spectroscopic studies of KCP(Br), KCP(Cl), and KTCP[33] and are now actively searching for the metal–metal vibration in these and newly prepared partially oxidized salts.

A rather striking correlation is that which can be made between Pt–Pt separations and the torsion angles formed by adjacent platinocyanide groups in these chain forming, but *not* necessarily partially oxidized, salts. Adjacent platinocyanide

Table VI. The Pt–Pt Bond Distance as a Function of Torsion Angle between Adjacent Platinocyanide Groups Forming Pt Atom Chains

Compd	Pt oxidation no.	Pt–Pt distance, Å	Torsion angle, deg	Ref
$Na_2[Pt(CN)_4]\cdot 3H_2O$	2.0	3.65, 3.75	0	36
$K_2[Pt(CN)_4]\cdot 3H_2O$	2.0	3.48	15.7–16.7	7
$NaK[Pt(CN)_4]\cdot 3H_2O$	2.0	3.25	36	21
$K_{1.75}[Pt(CN)_4]\cdot 1.5H_2O$	2.25	2.96	38.5–51.8	This work
$K_2[Pt(CN)_4]Br_{0.3}\cdot 3H_2O$	2.33	2.89	45	3

groups within a Pt–Pt chain apparently reach a repulsive energy minimum between CN π clouds, when the Pt–Pt separation is very short, by forming a completely staggered (45° Pt–CN torsion angle) configuration as observed in KCP(Br). A rather smooth relationship between Pt–Pt separation and torsion angle is observed as given in Table VI. It is then entirely plausible that the strong $K^+\cdots{}^-N{\equiv}C$ interactions in K(def)TCP cause a rotation of the Pt(2)$(CN)_4^{-1.75}$ group about the Pt(1)–Pt(2)–Pt(3) bond line. This in turn results in an *increase* in π–π cloud repulsion of adjacent CN groups thereby forcing expansion of the Pt–Pt separation. The correlation given in Table VI tends to support this hypothesis. In summary, it appears at this time that the Pt–Pt separations in K(def)TCP and KCP(Br) and the K^+ and Br^- contents, respectively, result from the complex interplay of electronic and stereochemical factors involving the Pt atoms. When the stereochemical factors are absent (no CN^- groups), the system may be expected to collapse into a Pt cluster with short Pt–Pt separations (<2.8 Å).

The crystallographic nonequivalence of the three Pt atoms in K(def)TCP does not eliminate the possibility that slight differences in valence could exist; however, essentially the same situation is observed in KCP(Br) and independent ESCA experiments[34,35] for the latter compound point to equivalent valence states. The equality of the Pt(1)–Pt(2) and Pt(2)–Pt(3) separations also argues in favor of equal valence states. This question is as yet unanswered in the case of K(def)TCP and as more of these unusual complexes are characterized by methods which allow determination of the Pt atom valence states, it should be possible to better correlate the DPO to the Pt–Pt separation. The C–N distances in K(def)TCP are all within one standard deviation of each other [1.158 (6) Å, see Table IVB] and agree perfectly with those in KCP(Br) and in unoxidized $K_2[Pt(CN)_4]\cdot 3H_2O$; hence there is little support for the suggestion that a transfer of electrons from cyanide to Pt occurs in the oxidized compounds.[34]

As we have stated previously,[7] ligands such as CN^-, CO, NO^+, and $(C_2O_4)^{2-}$ are small, form complexes with Pt which have square-planar coordination, and have excellent electron withdrawing tendencies. These are features that all combine to promote extended metal–metal Pt($5d_{z^2}$) orbital overlap and short Pt–Pt bonds. We previously rationalized the change in Pt–Pt distance from 3.48 Å in KTCP to 2.89 Å in KCP(X) almost solely in terms of electron configuration about Pt and it appears that these effects are still largely responsible for the Pt–Pt bond shortening to 2.96 Å in K(def)TCP. However, the overall Pt–Pt bond lengthening in K(def)TCP, compared to KCP(Br), results from unbalanced $K^+\cdots{}^-N{\equiv}C$ electrostatic interactions which, through transverse chain distortion and increased cyanide repulsions due to torsional rotation, cause reduced Pt($5d_{z^2}$) orbital overlap.

These results demonstrate that "Krogmann" type cyanoplatinate compounds form nonlinear Pt–Pt chains with equal metal–metal repeat separations even though they are not required crystallographically. There is as yet no evidence that the Pt chain deformation is caused by a charge density wave[37] or Peierls distortion[31] as in $K_2[Pt(CN)_4]Br_{0.3}\cdot H_2O$. It therefore appears that in the partially oxidized cyanoplatinates studied to date there are numerous factors in addition to the DPO which influence or determine the closeness of metal–metal atom approach and the extent to which metallic properties will develop. Electrostatic interactions of the type $K^+\cdots{}^-N{\equiv}C$ appear to be the most important factors causing either Pt chain "compression" or "distortion" in $K_2[Pt(CN)_4]Br_{0.3}\cdot 3H_2O$ and $K_{1.75}[Pt(CN)_4]\cdot 1.5H_2O$, respectively.

Our continuing studies involve the replacement of K^+ by other alkali metal ions to produce new cation deficient complexes. It seems likely that if no gross structural changes occur, and if the Pt–Pt chain remains intact, then an increase in distance of M^+ from the $C{\equiv}N^-$ groups will result in decreased $M^+\cdots{}^-N{\equiv}C$ electrostatic attraction and a concomitant decrease in Pt chain distortion. This could be accomplished by preparing the Rb^+ and Cs^+ derivatives. Conversely, attempts to prepare the Na^+ or Li^+ derivatives may result in such chain distortion that the complexes cannot be prepared. We are also experimenting with large monovalent organic cations which will hopefully produce even less Pt chain deformation. Alternatively the effect of coordinated cations may be decreased by increasing the size (transverse extent) of the Pt-coordinated ligands.

Acknowledgment. We wish to thank Drs. Paul L. Johnson, A. H. Reis, and S. W. Peterson for helpful discussions, Dr. Joel S. Miller for the loan of a $K_{1.75}[Pt(CN)_4]\cdot 1.5H_2O$ sample for powder diffraction characterization, J. P. Faris for emission spectrographic analyses which allowed us to determine sample purity, and Elizabeth Gebert for assistance with the powder x-ray diffraction experiments.

Registry No. $K_{1.75}Pt(CN)_4\cdot 1.5H_2O$, 59831-03-7.

Supplementary Material Available: Listing of structure factor amplitudes for $K_{1.75}[Pt(CN)_4]\cdot 1.5H_2O$ (13 pages). Ordering information is given on any current masthead page.

References and Notes

(1) This work was performed under the auspices of the U.S. Energy Research and Development Administration.
(2) Research participant sponsored by the Argonne Center for Educational Affairs from Middlebury College, Middlebury, Va.
(3) J. M. Williams, J. L. Petersen, H. M. Gerdes, and S. W. Peterson, *Phys. Rev. Lett.*, **33**, 1079 (1974); J. M. Williams, F. K. Ross, M. Iwata, J. L. Petersen, S. W. Peterson, S. C. Lin, and K. D. Keefer, *Solid State Commun.*, **17**, 45 (1975); J. M. Williams, M. Iwata, F. K. Ross, J. L. Petersen, and S. W. Peterson, *Mater. Res. Bull.*, **10**, 411 (1975); J. M. Williams, *Ferroelectrics.*, in press.
(4) J. M. Williams, M. Iwata, S. W. Peterson, K. A. Leslie, and H. J. Guggenheim, *Phys. Rev. Lett.*, **34**, 1653 (1975).
(5) K. D. Keefer, D. M. Washecheck, N. P. Enright, and J. M. Williams, *J. Am. Chem. Soc.*, **98**, 233 (1976).
(6) A. H. Reis, Jr., S. W. Peterson, D. M. Washecheck, and J. M. Miller, *J. Am. Chem. Soc.*, **98**, 234 (1976).
(7) D. M. Washecheck, S. W. Peterson, A. H. Reis, Jr., and J. M. Williams, *Inorg. Chem.*, **15**, 74 (1976).
(8) L. A. Levy, *J. Chem. Soc.*, 1081 (1912).
(9) T. R. Koch, N. P. Enright, and J. M. Williams, *Inorg. Synth.*, in press.
(10) K. Krogmann and H. D. Hausen, *Z. Naturforsch., B*, **23**, 1111 (1968).
(11) Private communication with Dr. J. S. Miller, Xerox Corporation, Webster, N.Y.
(12) M. J. Minot, J. H. Perlstein, and T. J. Kistenmacher, *Solid State Commun.*, **13**, 1319 (1973).
(13) All chemical analyses were performed by Midwest Microlab, Indianapolis, Ind.
(14) When viewing Figure 3 care must be exercised not to impose fourfold symmetry on the $Pt(CN)_4$ groups which are not square. Thus the angles we have termed torsion angles are the symmetry independent angles between $Pt(CN)_4$ groups.
(15) A. J. Zielen, P. Day, and J. M. Williams, Proceedings and Abstracts of Neutron Diffraction Meeting, Petten, The Netherlands, 1975, pp 38 and 39.
(16) The computer programs which were used in performing the necessary calculations, with their accession names in the World List of Crystallographic Computer Programs (3d ed), are as follows: data reduction and absorption corrections, DATALIB; data averaging and sort, DATASORT;

Fourier summation, FORDAP; least-squares refinement, OR XLFS3; error analysis of distances and angles, OR FFE3, and structural drawings, OR TEPII. For determination of least-squares planes the program PLNJO was used; J.-O. Lundgren, University of Uppsala, Uppsala, Sweden; based on the method of D. Blow, *Acta Crystallogr.*, **13**, 168 (1960). For the intensity statistics MULTAN was used; J. P. Declercq, G. Germain, P. Main, and M. M. Woolfson, *Acta Crystallogr., Sect. A*, **29**, 231 (1973). The Delauney-reduced cell parameters were derived using the computer program TRACER II, A Fortran Lattice Transformation-Cell Reduction Program, written by Dr. S. L. Lawton.
(17) P. Day and J. Hines, *Operating Systems Rev.*, **7**, 28 (1973).
(18) S. W. Peterson and H. A. Levy, *Acta Crystallogr.*, **10**, 70 (1957).
(19) (a) The Zachariasen approximation[19b] was used for the overall isotropic g parameter as defined and scaled by Coppens and Hamilton.[19c] The $|F_o|$ values were corrected for extinction from the expression $|F_o|_{corr} = |F_o|(1 + \bar{T}2g\lambda^3|F_c|^2/V^2 \sin 2\theta)^{-1/4}$, where $|F_c|$ is on an absolute scale, λ is the wavelength (Å), g is the refined extinction parameter, $\bar{T}$ is the mean absorption-weighted path length in the crystal in centimeters (calculated simultaneously during the computation of absorption corrections), and V is the unit cell volume (Å^3). (b) W. H. Zachariasen, *Acta Crystallogr.*, **23**, 558 (1967). (c) P. Coppens and W. C. Hamilton, *Acta Crystallogr., Sect. A*, **26**, 71 (1970).
(20) G. E. Bacon, *Acta Crystallogr., Sect. A*, **8**, 357 (1972).
(21) M. L. Moreau-Colin, *Bull. Soc. Fr. Mineral. Cristallogr.*, **91**, 332 (1968).
(22) K. Krogmann, *Angew Chem., Int. Ed. Engl.*, **8**, 35 (1969).
(23) Some very short Pt–Pt separations are: (a) 2.58 (1) Å in $[Pt_3(C_8H_{12})_3(SnCl_3)_2]$, L. J. Guggenberger, *Chem. Commun.*, 512 (1968); (b) 2.581 Å in $[Pt_2(\pi\text{-}C_5H_5)_4]$, K. K. Cheung, R. J. Cross, K. P. Forrest, R. Wardle, and M. Mercer, *Chem. Commun.*, 875 (1971); (c) 2.675 (1) Å in $Pt_3[P(C_6H_{11})_3]_4(CO)_3$, A. Albinati, G. Carturan, and A. Musco, *Inorg. Chim. Acta*, **16**, L3-L4 (1976); (d) 2.647 Å in $[Pt_2S(CO)(PPh_3)_3]$, A. C. Skapski and P. G. H. Troughton, *J. Chem. Soc. A*, 2772 (1969); and (e) J. M. Williams, *Inorg. Nucl. Chem. Lett.*, **12**, 651 (1976).
(24) P. L. Johnson, T. R. Koch, J. A. Abys, and J. M. Williams, to be published.
(25) K. Krogmann, *ACS Symp. Ser.*, **5**, (1974).
(26) J. Bernasconi, P. Brüesch, D. Kuse, and H. R. Zeller, *J. Phys. Chem. Solids*, **35**, 145 (1974).
(27) R. L. Musselman, T. R. Koch, and J. M. Williams, to be published.
(28) T. W. Thomas, C.-H. Hsu, M. M. Labes, P. S. Gomm, A. E. Underhill, and D. M. Watkins, *J. Chem. Soc., Dalton Trans.*, 2050 (1972).
(29) K. Carneiro, J. Eckert, G. Shirane, and J. M. Williams, *Solid State Commun.*, in press.
(30) A. J. Schultz, G. D. Stucky, and J. M. Williams, to be published.
(31) R. Comes, M. Lambert, H. Launois, and H. R. Zeller, *Phys. Rev. B*, **8**, 571 (1973); R. Comes, M. Lambert, and H. R. Zeller, *Phys. Status Solidi B*, **58**, 587 (1973).
(32) L. Pauling, "The Nature of the Chemical Bond", 3d ed, Cornell University Press, Ithaca, N.Y., 1960.
(33) J. R. Ferraro, L. J. Basile, and J. M. Williams, *J. Chem. Phys.*, **64**, 732 (1976).
(34) D. Cahen and J. E. Lester, *Chem. Phys. Lett.*, **18**, 108 (1973).
(35) M. A. Butler, D. L. Rousseau, and D. N. E. Buchanan, *Phys. Rev. B*, **7**, 61 (1973).
(36) P. L. Johnson, T. R. Koch, and J. M. Williams, to be published.
(37) C. F. Eagen, S. A. Werner, and R. B. Saillant, *Phys. Rev. B*, **12**, 2036 (1975). Note that the charge density wave distortions in KCP(Br) are small and the rigid sinusoidal displacement of the $Pt(CN)_4^{-2}$ groups (at 7 K) amounts to only 0.026 Å.

Contribution from the Chemistry Division, Argonne National Laboratory, Argonne, Illinois 60439, and the Webster Research Center, Xerox Corporation, Webster, New York 14580

The Nature of the Pt Chain Distortion in the Partially Oxidized One-Dimensional Complex, $K_{1.75}Pt(CN)_4 \cdot 1.5H_2O$[1]

A. H. REIS, Jr., S. W. PETERSON,* D. M. WASHECHECK,[2] and JOEL S. MILLER[3]

Received March 22, 1976 AIC60199Y

The oxidation of potassium tetracyanoplatinate(II) in the absence of halide ions results in the formation of bronze needles of $K_{1.75}Pt(CN)_4 \cdot 1.5H_2O$ stoichiometry. The structure of this partially oxidized material consists of parallel one-dimensional noncollinear chains involving a commensurate repeat unit of 11.865 Å. Thus the unit cell contents as deduced from single crystal x-ray data is formulated $K_7[Pt(CN)_4]_4 \cdot 6H_2O$ and is stoichiometric. This material crystallizes in the triclinic space group $P\bar{1}$ with a = 10.323 (14), b = 9.285 (13), c = 11.865 (17) Å, α = 77.31 (3), β = 114.85 (5), γ = 73.84 (2)°, and Z = 4. The structure was solved by a combination of Patterson, Fourier, and least-squares refinement techniques to an R_F = 0.050 for the 1840 observed reflections for which $F_o > 3\sigma F_o$. There are three inequivalent Pt atoms in the chain and two Pt–Pt bond distances of 2.967 (1) and 2.976 (1) Å. The average twist angles of the cyanide ligands of the tetracyanoplatinate planes are 45.3 (5) and 49.8 (3.7°). An extensive network of K^+ ionic bonding and hydrogen bonded water molecules knit the material together orthogonal to the chain direction. The chain distortion is shown to be due to Coulombic forces acting between the tetracyanoplatinate anions, located in the asymmetric crystal sites at $z = \sim 1/4$ and $3/4$, and the coordinated asymmetric K^+ distribution. The crystallographic analysis leads to the formal oxidation state of +2.25 for Pt in this potassium deficient material and an odd number of electrons per unit cell.

Introduction

In recent years there has been an enhanced interest in the chemical and physical properties of pseudo-one-dimensional inorganic and organic complexes due to the prediction and observation of a number of unusual anisotropic physical phenomena[4-6] (e.g., high conductivity, metallic state, metal insulator transition, charge density wave, superconductivity) and chemical properties (e.g., novel structures containing infinite chains with short interplanar spacings, homogeneous nonstoichiometric compositions, and mixed valency) directly associated with the reduced dimensionality of various one-dimensional systems.[6-8]

For these reasons there has been immense interest in the synthesis and characterization of several partially oxidized one-dimensional materials. The best characterized highly conducting one-dimensional complexes are based on the partial oxidation of tetracyanoplatinate(II) and reduction of 7,7,-8,8-tetracyano-*p*-quinodimethane.[6] Partial oxidation of tetracyanoplatinate(II) in the presence of chloride or bromide results in the formation of $K_2Pt(CN)_4X_{0.3} \cdot 3H_2O$ (X = Cl, Br) which are well characterized at several temperatures by x-ray,[9-10] neutron,[11-14] and diffuse scattering[15] methods and have an incommensurate superlattice which is attributed to a charge density wave instability.[16]

Oxidation of tetracyanoplatinate(II) in the absence of halide ions was shown by Levy in 1910[17] to yield a complex of nominal $K_{1.75}Pt(CN)_4 \cdot 1.5H_2O$[17,18] stoichiometry. This bronze material was initially characterized by short interplanar spacings from x-ray powder analysis[18] and conductivity[19] which increased with decreasing temperature[19a] thereby suggesting a metallic state. With the isolation of single crystals suitable for x-ray[20] and neutron[21] analysis the structural determination of this partially oxidized cation deficient complex of $K_{1.75}Pt(CN)_4 \cdot 1.5H_2O$, KDEF, has been completed. We are presenting here the results of the complete structural investigation which has been undertaken to characterize the nature of this cation deficient partially oxidized material and determine the driving force behind the Pt chain distortion.

Experimental Section

Crystal Preparation. KDEF was prepared by the partial oxidation of $K_2Pt(CN)_4 \cdot 3H_2O$ in acid solution with hydrogen peroxide according